Synthesis of Novel Mixed Metal Cluster Complexes of Osmium and Mercury: Formation of the Wheel-Shaped Cluster Complexes $Os_6(\mu_6\text{-}Hg)(\mu\text{-}PR_2)_2(CO)_{20}$ (R = Ph, *i*-Bu)

Hans Egold,* Markus Schraa, Ulrich Flörke, and Janusch Partyka

Anorganische und Analytische Chemie der Universität Paderborn, Fachbereich 13, Chemie und Chemietechnik, Warburgerstr. 100, D-33098 Paderborn, Germany

Received December 14, 2001

The reaction of $[PPN][Os_3(\mu\text{-}PR_2)(CO)_{10}]$ (R = Ph **1a**, *i*-Bu **1b**) with $HgCl_2$ in THF at −90 °C under exclusion of light gave the spirocyclic cluster $\mu_4\text{-}Hg[Os_3(\mu\text{-}PR_2)(\mu\text{-}CO)(CO)_9]_2$ (R = Ph **2a**, *i*-Bu **2b**). In these compounds the μ_4-Hg bridges one Os−Os edge of each Os_3 subunit. The remaining four edges are bridged by the μ-CO and μ-PPh_2 ligands, respectively. ^{13}C NMR spectra of ^{13}CO-enriched **2a** recorded at room temperature indicate an intramolecular rotation of the Os_3 subunits around the axis running through the mercury atom and the midpoints of the Os−Os vectors it bridges. When **2a** is heated in toluene or 1,4-dioxane, a rearrangement of the metal skeleton takes place. The μ_4-Hg moiety is shifted to another edge of one of the Os_3 rings, giving the isomer $(CO)_{10}(\mu\text{-}PPh_2)Os_3(\mu_4\text{-}Hg)Os_3(\mu\text{-}PPh_2)(\mu\text{-}CO)(CO)_9$, **3a**. The kinetics of this process were measured by UV/vis spectroscopy at four different temperatures in toluene and 1,4-dioxane, respectively. The reaction is of first order with a rate constant of $6.66(2) \times 10^{-5}$ s^{-1} in toluene at 331.6(1) K. The thermodynamic parameters $\Delta H^{\ddagger} = 97(5)$ kJ mol^{-1}, $\Delta S^{\ddagger} = -33(13)$ J K^{-1} mol^{-1}, and $\Delta G^{\ddagger} = 107(6)$ kJ mol^{-1} were derived from an Eyring plot. The analogous cluster complex **3b** with μ-P(*i*-Bu)$_2$ bridges has been obtained, too. Its structure has been confirmed by single-crystal X-ray analysis. **2a** and **2b** are highly photosensitive in solution. Upon exposure to daylight, they rearrange to give the novel wheel-shaped cluster complexes $Os_6(\mu_6\text{-}Hg)(\mu\text{-}PR_2)_2(CO)_{20}$ (R = Ph **4a**, *i*-Bu **4b**). The structure of **4a** was confirmed by single-crystal X-ray analysis. In **4a** the Hg atom is located at the center of a Os_6 ring. The ring is corrugated with the mercury atom in bonding distance to all osmium atoms. The course of the reaction was monitored for the conversion of **2a** by UV/vis spectra exhibiting two isosbestic points indicating an intramolecular reaction.

Introduction

In heptanuclear mixed metal cluster complexes with a spirocyclic $M_3(\mu_4\text{-}Hg)M_3$ (M = Ru,[1−6] Os[4,7−10]) framework a mercury atom links two M_3 cluster subunits. This type of compound is usually easy to prepare by metathesis or redistribution reactions, respectively. For example the cluster $\mu_4\text{-}Hg[Os_3(\mu\text{-}H)(\mu_3\text{-}S)(CO)_{10}]_2$ was synthesized in 80% yield by salt metathesis of HgI_2 with $[PPN][Os_3(\mu\text{-}H)(\mu_3\text{-}S)(CO)_8)]$.[4] The resulting heptanuclear cluster complexes are very dynamic molecules due to the flexible bonding properties of the mercury atom which binds to the M_3 cluster subunits via a linear spd[5] manifold.[11−13] The dynamic properties are related to two different processes, the first one being an intramolecular rotation about an axis running through the mercury atom and the midpoints of the two M−M bonds it bridges.[3,14,15] The second process is based on an intramolecular exchange process in which motion of the μ_4-Hg moiety averages two or all M−M vectors of the M_3 subunits.[3−4,14,15] So far an isomerization of the above-described class of clusters giving μ_6-bound mercury has not been observed, but Rosenberg et al. propose a sandwich-like intermediate $Ru_3(\mu_6\text{-}Hg)Ru_3$ for the rearrangement of $\mu_4\text{-}Hg[Ru_3(\mu_3\text{-}\eta^2\text{-}C_2(t\text{-}Bu))(CO)_9]_2$ in solution.[3] In general a μ_6-bonding mode is rare for mercury and usually found in clusters dominantly built of Hg and Pt or Pd atoms, respectively.[16−25] In these closed

(1) Ermer, S.; King, K.; Hardcastle, K. I.; Rosenberg, E.; Lanfredi, A. M. M.; Tiripicchio, A.; Tiripicchio-Camellini, M. *Inorg. Chem.* **1983**, *22*, 1339.
(2) Gomez-Sal, M. P.; Johnson, B. F. G.; Lewis, J.; Raithby, P. R.; Syed-Mustaffa, S. N.; Azman B. *J. Organomet. Chem.* **1984**, *272*, C21.
(3) Hajela, S.; Novak, B. M.; Rosenberg, E. *Organometallics* **1989**, *8*, 468.
(4) Rosenberg, E.; Hardcastle, K. I.; Day, M. W.; Gobetto, R.; Hajela, S.; Muftikian, R. *Organometallics* **1991**, *10*, 203.
(5) Andreu, P. L.; Cabeza, J. A.; Llamazares, A.; Riera, V.; Bois, C.; Jeannin, Y. *J. Organomet. Chem.* **1991**, *420*, 431.
(6) Osella, D.; Milone, L.; Kukharenko, S. V.; Strelets, V. V.; Rosenberg, E.; Hajela, S. *J. Organomet. Chem.* **1993**, *451*, 153.
(7) Au, Y.-K.; Wong, W.-T. *J. Chem. Soc., Dalton Trans.* **1995**, 1389.
(8) Au, Y.-K.; Wong, W.-T. *J. Chem. Soc., Dalton Trans.* **1996**, 899.
(9) Au, Y.-K.; Wong, W.-T. *Inorg. Chem.* **1997**, *36*, 2092.
(10) Kong, F.-S.; Wong, W.-T. *J. Chem. Soc., Dalton Trans.* **1999**, 2497.
(11) Gade, L. H. *Angew. Chem.* **1993**, *105*, 25.
(12) King, R. B. *Polyhedron* **1988**, *7*, 1813.
(13) King, R. B. *J. Chem. Inf. Comput. Sci.* **1994**, *34*, 410.
(14) Bianchini, A.; Farrugia, L. J. *Organometallics* **1992**, *11*, 540.
(15) Farrugia, L. J. *Chem. Commun.* **1987**, 147.
(16) Yamamoto, Y.; Yamazaki, H.; Sakurai, T. *J. Am. Chem. Soc.* **1982**, *104*, 2329.
(17) Albinati, A.; Moor, A.; Pregosin, P. S.; Venanzi, L. M. *J. Am. Chem. Soc.* **1982**, *104*, 7672.

10.1021/om0110585 CCC: $22.00
Publication on Web 04/02/2002

Scheme 1

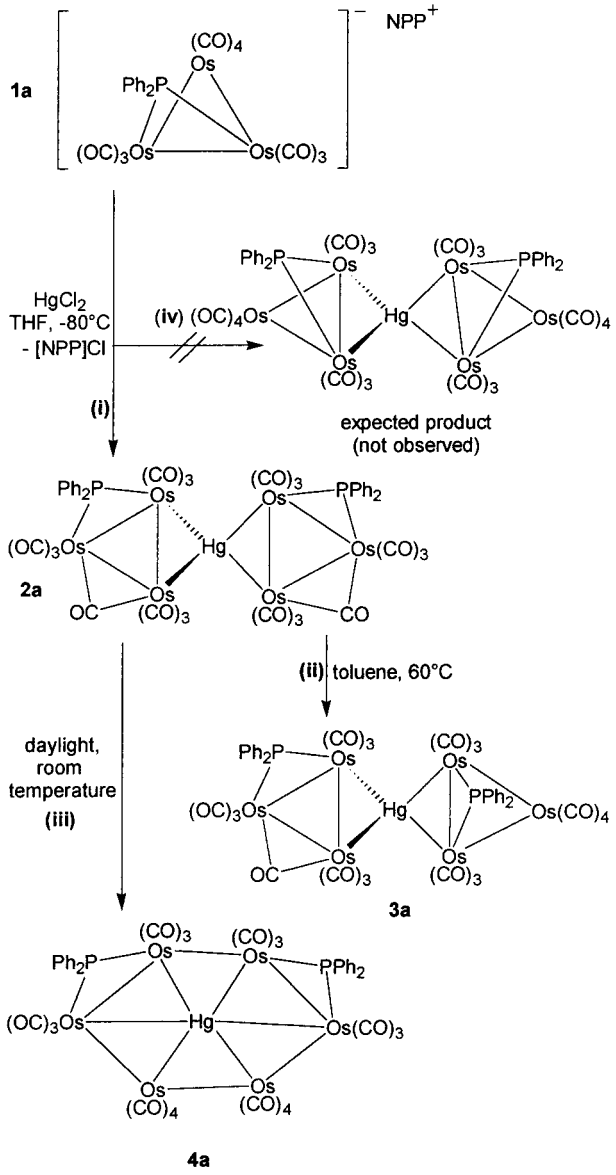

cluster compounds the Hg atom occupies the center of a trigonal prism built of Pt or Pd atoms, respectively. So far there are only five cluster complexes known in which a μ_6-Hg atom is linked to metal atoms other than Pt or Pd, respectively.[26−30] In this paper we wish to report the synthesis of another cluster of the latter kind by photochemical conversion of a heptanuclear mixed Os−Hg cluster complex with a spirocyclic $Os_3(\mu_4\text{-Hg})Os_3$ core. Furthermore the thermal isomerization of the latter compound has been investigated by UV spectroscopy, and the kinetic data obtained are discussed with respect to the mechanism of the reaction.

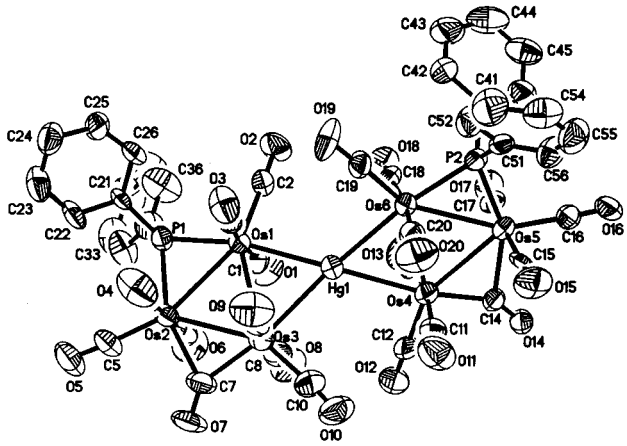

Figure 1. Molecular structure of **2a** with 50% probability ellipsoids. Hydrogen atoms are omitted.

Results and Discussion

On dropwise addition of 2 equiv of yellow [PPN][Os_3-(μ-PR_2)$(CO)_{10}$] (R = Ph **1a**, *i*-Bu **1b**) dissolved in THF to a solution of $HgCl_2$ in THF at −90 °C, a deep red reaction mixture was obtained. After heating to room temperature and working up in both cases a mixture of three mixed Os/Hg cluster complexes was obtained. The compounds could not be separated by TLC, but pure samples of these clusters were obtained by fractional crystallization. Comparison of the ^{31}P NMR data of the obtained pure cluster complexes with ^{31}P NMR data of the mixtures prior to fractional crystallization proves that pure samples of all compounds present in the mixtures were isolated. Four of these cluster complexes were characterized by single-crystal X-ray analysis.

1. Primary Spirocyclic Condensation Products 2a and 2b. The first type of cluster complex isolated from the above-mentioned reaction mixtures is the novel spirocyclic heptanuclear cluster complex μ_4-Hg[Os_3(μ-PR_2)(μ-CO)$(CO)_9]_2$ (R = Ph **2a**, *i*-Bu **2b**) (Scheme 1, step i). These compounds exhibit a single ^{31}P resonance at δ = 216.6 for R = Ph and δ = 189.1 for R = *i*-Bu, respectively. The presence of μ-CO ligands in solution is confirmed by ν(CO) absorption spectra showing weak absorptions at 1803 cm^{-1} for **2a** and 1813 cm^{-1} for **2b**, respectively. ^{31}P NMR spectra of the reaction mixture of **1a** with $HgCl_2$ recorded at −60 °C show only resonances of **2a**, indicating that cluster complexes **2a** and **2b**, respectively, are the primary condensation products.

Molecular Structures of 2a and 2b. The molecular structures of **2a** (Figure 1) and **2b** (not depicted) were determined by single-crystal X-ray analysis. The molecules both exhibit an $Os_3(\mu_4\text{-Hg})Os_3$ metal core. They are largely isostructural but differ in the substitution

(18) Mednikov, E. G.; Eremenko, N. K.; Bashilov, V. V.; Sokolov, V. I. *Inorg. Chim. Acta* **1983**, *76*, L31.
(19) Yamamoto, Y.; Takahashi, K.; Yamazaki, H. *Chem. Lett.* **1985**, 201.
(20) Yamamoto, Y.; Yamazaki, H. *J. Chem. Soc., Dalton Trans.* **1989**, 2161.
(21) Tanase, T.; Horiuchi, T.; Yamamoto, Y.; Kobayashi, K. *J. Organomet. Chem.* **1992**, *440*, 1.
(22) Yamamoto, Y.; Yamazaki, H. *Organometallics* **1993**, *12*, 933.
(23) Yamamoto, Y.; Yamazaki, H *Inorg. Chim. Acta* **1994**, *217*, 121.
(24) Hao, L.; Vittal, J. J.; Puddephatt, R. J. *Inorg. Chem.* **1996**, *35*, 269.
(25) Hao, L.; Vittal, J. J.; Puddephatt, R. J. *Organometallics* **1996**, *15*, 3115.
(26) Jones, R. A.; Mayor R. F.; Wilkinson, G.; Galas, A. M. R.; Hursthouse, M. B. *J. Chem. Soc., Dalton Trans.* **1981**, 126.
(27) Braunstein, P.; Rose, J.; Tiripicchio, A.; Tiripicchio-Camellini, M. *Angew. Chem.* **1985**, *97*, 761.
(28) Braunstein, P.; Rose, J.; Tiripicchio, A.; Tiripicchio-Camellini, M. *J. Chem. Soc., Dalton Trans.* **1992**, 911.
(29) Gade, L. H.; Johnson, B. F. G.; Lewis, J.; McPartlin, M.; Scowen, I. J. *J. Chem. Soc., Dalton Trans.* **1996**, 597.
(30) Charadonna, G.; Ingrosso, G.; Marchetti, F. *Angew. Chem., Int. Ed.* **2000**, *39*, 3872.

of the μ-P bridge atoms with phenyl residues for **2a** and isobutyl residues for **2b**.

2a shows a central spirocyclic μ_4-Hg atom which connects two Os_3 ring moieties, Os1−Os3 and Os4−Os6, both with equal ligand arrangements. Each osmium atom is attached to three terminal CO ligands, of which two are in axial and one in equatorial position. The three Os−Os bonds of each ring fragment are bridged by the different groups μ-CO, μ-PCy_2, and μ-Hg. All these bridging atoms lie in the Os_3 planes; the deviations from the planes range from −0.08(2) to 0.10(1) Å. With respect to the metal framework the two μ-PCy_2 ligands are in *syn* position to each other, as are the μ-CO groups. These ligand arrangements lead to slightly distorted square pyramidal coordination of each Os atom with the equatorial CO groups in the apical positions. With respect to the two additional Os−Os bonds all osmium atoms show a 7-fold coordination pattern which may be described as distorted pentagonal bipyramidal. All Os−Os distances differ significantly, at 2.9738(13) (Os1−Os3), 2.9623(12) (Os5−Os6), 2.9510(13) (Os4−Os6), 2.9483(15) (Os1−Os2), 2.9252(16) (Os4−Os5), and 2.8937(14) Å (Os2−Os3), respectively. The two shortest bonds are bridged by the μ-CO groups. The Hg−Os distances are also different, at 2.8871(13) (Os4), 2.8542(15) (Os3), 2.8223(13) (Os1), and 2.8109(15) Å (Os6). The two shorter bonds are *trans* to the two Os−P vectors and the longer ones *trans* to the Os−μ-CO vectors. The coordination of the Hg atom deviates strongly from ideal spirocyclicity with an $Os_2Hg/HgOs_2$ angle of 46.29(4)° instead of 90°. The μ-P bridges are symmetric with average Os−P bond lengths of 2.321(6) Å, but the μ-CO groups show one short and one long Os−C bond with average values of 2.03(2) and 2.29(2) Å, respectively. The structural unit of a spirocyclic mercury atom linked to two Os3 rings is known from $(\mu_4\text{-Hg})[Os_3(\mu\text{-H})(\mu_3\text{-S})(CO)_9]_2$,[4] $(\mu_4\text{-Hg})[Os_3(\mu\text{-Cl})(CO)_{10}]_2$,[9] and $(\mu_4\text{-Hg})[Os_3(\mu\text{-SR})(CO)_{10}]_2$.[10] However, in contrast to the planar $HgOs_3$ unit of **2a** these molecules show butterfly-type Os_3Hg cores. Nevertheless Hg−Os bond lengths in these structures range from 2.815(2) to 2.903(3) Å and compare well with those of **2a**.

Though being isostructural to **2a** with respect to the overall ligand arrangement, the compound **2b** shows significant changes of the metal framework concerning the μ_4-Hg atom, which has now almost ideal spirocyclic coordination with an $Os_2Hg/HgOs_2$ angle of 84.93(3)°. The bridging μ-P and μ-CO groups still lie in the Os_3 planes with deviations from these planes between 0.005(5) and 0.051(5) Å. Hg−Os bond lengths range from 2.8605(12) to 2.7774(10) Å and the Os−Os distances from 2.8901(12) to 2.9820(12) Å.

Mechanistic Aspects. The formation of this type of cluster complex is most surprising, as mercury in heptanuclear cluster complexes with $Os_3(\mu_4\text{-Hg})Os_3$ core is known to bridge the Os−Os bonds already bridged by a three-electron-donor ligand only.[8−10] Therefore we initially expected the formation of an analogous cluster complex with mercury bridging the phosphido-bridged Os edge (Scheme 1, step iv). However, this type of product was not observed at all. Interestingly the condensation of **1a** with $ClMPPh_3$ (M = Cu, Ag, Au) instead of $HgCl_2$ proceeds as expected, giving the tetranuclear cluster complexes $Os_3(MPPh_3)(\mu\text{-}PPh_2)(CO)_{10}$ in which the coinage metal bridges the Os−Os bond bridged by phosphorus.[42] We assume that the formation of **2a** and **2b** proceeds kinetically controlled. An analogous cluster complex may be formed in the initial step of the reaction of **1a** with $ClMPPh_3$ too, but if that is true, it rapidly isomerizes to give the thermodynamically more stable cluster complex with gold bridging the phosphido-bridged Os−Os bond. This idea is supported by the example of $Os_3(AuPEt_3)(\mu\text{-}\eta^3\text{-}C_3H_5)(CO)_{10}$, in which the allylic moiety bridges one Os−Os edge and $AuPEt_3$ another.[31]

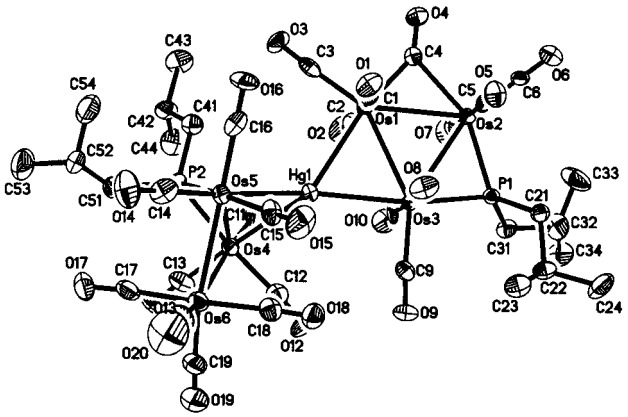

Figure 2. Molecular structure of **3b** with 50% probability ellipsoids. Hydrogen atoms are omitted.

2. Formation of 3a and 3b by Thermal Rearrangement of 2a and 2b, Respectively. The above proposed metal shift from one Os−Os edge to another can be observed for both **2a** and **2b**. Both cluster complexes rearrange on heating under complete exclusion of daylight, giving $(CO)_{10}(\mu\text{-}PR_2)Os_3(\mu_4\text{-Hg})Os_3(\mu\text{-}PR_2)(\mu\text{-CO})(CO)_9$ (R = Ph **3a**, *i*-Bu **3b**) (Scheme 1, step ii). Compared to **2a** and **2b** in these cluster complexes, the mercury is shifted to one of the phosphido-bridged Os−Os edges. This has been confirmed by X-ray analysis of a single crystal of **3b** (Figure 2).

Molecular Structure of 3b. Complex **3b** combines two different Os_3 patterns. The Os1−Os3 group is the same as that known from **2a** and **2b** with bridging μ-P(*i*-Bu_2) and μ-CO ligands and the μ_4-Hg atom. These lie in the Os_3 plane with deviations from −0.076(3) to 0.055(1) Å. The Os−Os bond lengths are 2.8974(9) (Os1−Os2), 2.9543(8) (Os1−Os3), and 2.9561(8) Å (Os2−Os3), respectively, and the shortest one is again bridged by the carbonyl ligand. The coordination of the Hg atom with Hg−Os distances of 2.7971(9) (Os3), 2.8996(8) (1), 2.8448(8) (4), and 2.8518(10) Å (5) deviates from ideal spirocyclicity with an $Os_2Hg/HgOs_2$ angle of 68.43(4)°. The Os4−Os6 group shows a different ligand coordination pattern. Os4 and Os5 each are attached to three and Os6 to four terminal CO ligands. The Os4−Os5 bond of 2.9596(11) Å is doubly bridged by the Hg atom and a μ-P(*i*-Bu_2) group, but the two Os4−Os6 and Os5−Os6 bonds of 2.8964(12) and 2.8873(9) Å, respectively, are not bridged. This $HgOs_3$ moiety has a butterfly-type structure with an Os_3/Os_2Hg opening angle of 125.54(3)°, and the Os_2P plane halves this butterfly with $HgOs_2/Os_2P$ and Os_3/Os_2P angles of 62.97(9)° and 62.57-

(31) Housecroft, C. E.; Johnson, B. F. G.; Lewis, J.; Lunniss, J. A.; Owen, S. M.; Raithby, P. R. *J. Organomet. Chem.* **1991**, *409*, 271.

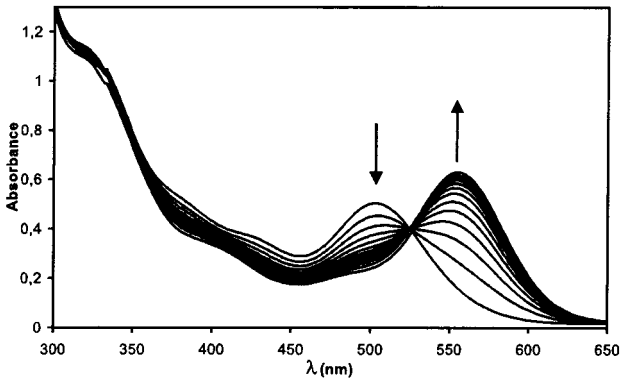

Figure 3. Time-resolved UV/vis spectra for the rearrangement **2a** → **3a** at 58.4 °C in toluene.

Table 1. Rate Constants and Thermodynamic Data of the Rearragement 2a → 3a

temp [K]	solvent	rate constant [1/s]	thermodynamic data
331.6(1)	toluene	$6.66(2) \times 10^{-5}$	
342.9(1)	toluene	$2.501(1) \times 10^{-4}$	$\Delta H^{\ddagger}$ =97(5) kJ/mol
352.6(1)	toluene	$6.63(2) \times 10^{-4}$	$\Delta S^{\ddagger} = -34(13)$ J/(K mol)
363.1(1)	toluene	$1.504(5) \times 10^{-3}$	$\Delta G^{\ddagger} = 107(6)$ kJ/mol
331.6(1)	1,4-dioxane	$3.815(11) \times 10^{-5}$	
342.9(1)	1,4-dioxane	$1.646(5) \times 10^{-4}$	$\Delta H^{\ddagger} = 103(6)$ kJ/mol
352.6(1)	1,4-dioxane	$4.391(16) \times 10^{-4}$	$\Delta S^{\ddagger} = -19(16)$ J/(K mol)
363.1(1)	1,4-dioxane	$1.07(2) \times 10^{-3}$	$\Delta G^{\ddagger} = 109(7)$ kJ/mol

(9)°. The structure of this Os_3 unit compares well with the butterfly geometries of the complexes cited above.

The ^{31}P NMR spectra of **3a** and **3b** prove the existence of two different phosphido bridges. For example **3a** shows ^{31}P NMR resonances at $\delta = 209.7$ and $\delta = 43.9$. As a result of comparison with the data of **2a**, the chemical shift of the resonance at low field must be assigned to the phosphorus bridging an Os−Os edge not bridged by mercury. Consequently the latter resonance must be assigned to the other phosphorus bridging the same edge as mercury.

Kinetics and Thermodynamic Data. **3a** and **3b** are the second type of cluster isolated from the mixture resulting from the reaction of **1a** and **1b**, respectively, with $HgCl_2$. Hence the isomerization of **2a** and **2b** giving **3a** and **3b**, respectively, already takes place at room temperature. Nevertheless according to ^{31}P NMR spectra recorded from the reaction mixtures, **3a** and **3b** are formed in low yield. This observation is in good agreement with the thermodynamic parameters of isomerization. The latter were determined for the rearrangement of **2a**. The course of the reaction was followed by UV/vis spectroscopic measurements at 58.4, 69.7, 79.4, and 89.9 °C in toluene and 1,4-dioxane, respectively. In Figure 3 time-dependent UV/vis spectra of the reaction in toluene at 58.4 °C are depicted. The course of the reaction was monitored for 12 h. During this period of time the absorption maximum of **2a** at 500 nm slowly decreases. Meanwhile the absorption band at 554 nm belonging to **3a** is slowly increasing. At 525 nm an isosbestic point is observed indicating a unitary course of reaction. At longer reaction times the isosbestic point is lost due to decomposition reactions. Therefore the extinctions at t equals infinity, $E_{\lambda\infty}$, could not be determined. Assuming an intramolecular rearrangement,[4,11] the time-dependent extinction data were analyzed by formal integration,[32] giving a rate law of first order and a rate constant for each temperature (Table 1). The temperature dependence of the rate constants was investigated by an Eyring plot (Figure 4) giving the thermodynamic data of this reaction (Table 1). As can be seen from Table 1, the thermodynamic activation parameters are with respect to the large standard deviation independent from the solvent used. $\Delta G^{\ddagger}$ amounts 107(6) kJ mol^{-1} in toluene, explaining the low yield of **3a** and **3b** due to their slow formation at room temperature. The value of $\Delta S^{\ddagger}$ is negative or at least close to zero, strongly indicating an intramolecular isomerization without dissociative steps. There are two possible mechanisms for this isomerization. Either the μ_4-Hg is shifted to the phosphido-bridged Os−Os edge or the phosphido bridge is shifted from one edge to another. Apparently these data give no clear hint on the pathway, but comparison with other $M_3(\mu_4\text{-Hg})M_3$ systems supports the idea of mercury shifting from one edge to another.[4,11]

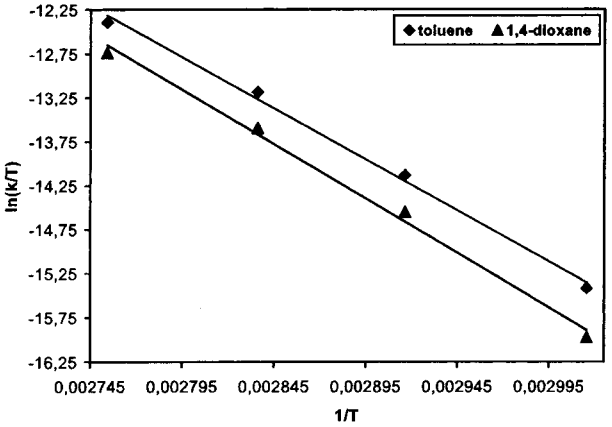

Figure 4. Eyring plot for the rearrangement **2a** → **3a**.

Photochemical Formation of Wheel-Shaped Cluster Complexes 4a and 4b. The last type of cluster complex isolated from the reaction of **1a** and **1b** with $HgCl_2$ is the wheel-shaped $Os_6(\mu_6\text{-Hg})(\mu\text{-}PR_2)_2(CO)_{20}$ (R = Ph **4a**, *i*-Bu **4b**).

Molecular Structure of 4a. The molecular structure of **4a** (Figure 5) was determined by single-crystal X-ray analysis. The latter shows a completely new structure type with a 6-fold coordinated mercury atom in the center of an Os_6 ring. This ring unit is not planar but rather twisted. The deviations of Os atoms from the best plane through this metal arrangement with Hg lying in the plane range from −0.852(1) to 0.839(1) Å. Atoms Os1 to Os4 are attached to three terminal CO ligands each, two in axial and one in equatorial position. Additionally Os1 and Os2 as well as Os3 and Os4 are bridged by μ-PPh_2 groups, and Os5 and Os6 are attached to four terminal carbonyl groups. Each Os atom thus reaches a 7-fold coordination from four nonmetal ligands, two neighboring osmium atoms and the central Hg atom, which can best be described as a distorted pentagonal bipyramid with the two CO groups at the apexes. The short Hg−Os1 and Hg−Os4 bond lengths of 2.8583(12) and 2.8598(13) Å include a nearly linear Os1−Hg−Os4 angle of 172.80(4)°. This structural fea-

(32) Mauser, H. *Experimentelle Methoden der Physik und Chemie (Band 1): Formale Kinetik*; Bertelsmann Universitätsverlag, 1974.

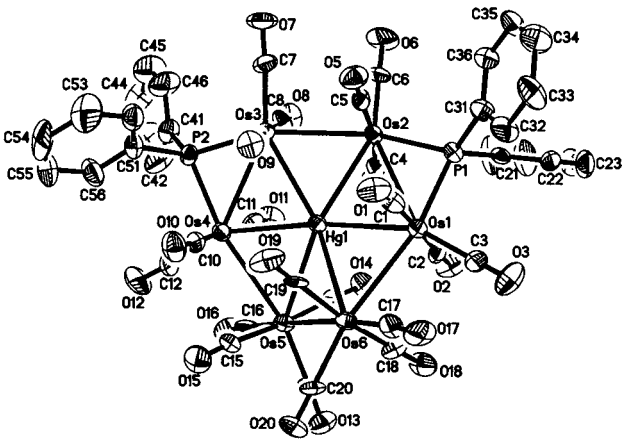

Figure 5. Molecular structure of **4a** with 50% probability ellipsoids. Hydrogen atoms are omitted.

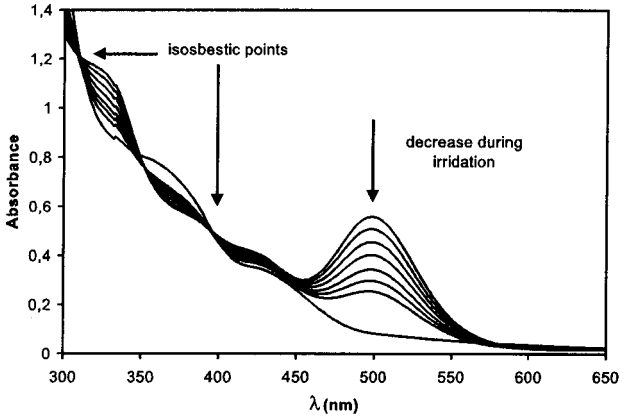

Figure 6. Time-resolved UV/vis spectra of the photochemical rearrangement **2a** → **4a**.

ture is probably indicating that mercury is strongly bonding along this axis via a linear spd[5] manifold.[11−13] All other Os−Hg bond lengths are significantly longer, and their Os−Hg−Os angles are far from linear. Two medium bonds of 2.8969(13) and 2.9097(13) Å are directed to Os2 and Os3, respectively, which make the shortest Os−Os bond of 2.9656(12) Å. All other Os−Os bond lengths range from 3.0576(14) to 3.1023(15) Å. The two longest Hg−Os bonds are those to Os5 (3.0683(13) Å) and Os6 (3.0506(15) Å). The accompanying Os−Hg−Os angles are Os2−Hg−Os5 152.16(4)° and Os3−Hg−Os6 152.68(4)°, both being clearly more acute than the Os1−Hg−Os4 angle. We propose that the interaction between Os2, Os3, Os5, Os6, respectively, and Hg is based on Os→Hg donor/acceptor bonds such as those found in $[Os_3(CO)_{11}Hg]_3$.[36] The latter exhibits short Os−Hg lengths of 2.717(4) Å due to strong σ-bonding and longer donor/acceptor bond lengths of 2.859(3) Å between $Os(CO)_4$ groups and Hg.

Investigation of the Photocyclization Process. The fascinating compounds **4a** and **4b** are formed in a photoreaction of **2a** and **2b**, respectively. The latter are very photosensitive in solution. For example a solution of **2a** in THF is converted by daylight at room temperature to give **4a** within 30 min (Scheme 1, step iii). The conversion of a solution of **2a** in THF (c = 0.043 mmol L^{-1}) was monitored by time-dependent UV/vis spectra. (Figure 6). The solution was irradiated by polychromatic light, and every 60 s a spectrum was recorded. After 6 min the solution was irradiated with more intense polychromatic light for another 10 min in order to complete the conversion. In the course of the reaction the intensity of the absorption band of **2a** at 489 nm rapidly decreased. In addition two isosbestic points are observed at 395 and 315 nm, indicating a unitary course of reaction[32,33] that most likely proceeds by an intramolecular rearrangement of the metal core. The final spectrum in the sequence recorded is that of pure **4a**, confirming complete conversion. Such a clean conversion is obtained only in highly diluted solution. In more concentrated solutions ($c \approx 1$ mmol L^{-1}) decomposition reactions occur as well, reducing the yield in preparative reactions to about 50%. To find out more about the photocyclization process, we decided to take a closer look at the educts **2a** and **2b**. Their molecular structures (compare structure discussions above) show dihedral angles $Os_2Hg/HgOs_2$ of 46.29(4)° and 84.93(3)°, respectively. The different angles indicated that the rings are able to rotate about an axis running through the mercury atom and the midpoints of the two Os−Os bonds it bridges. This hypothesis could be supported only by ^{13}C NMR spectra showing the resonances of the CO ligands.[4] Due to the low solubility of the compounds ($c_{max} \approx 1$ mmol L^{-1}), a ^{13}CO-enriched sample had to be prepared. The enrichment has been achieved by variation of a well-known reaction. On heating $Os_3(\mu\text{-H})(\mu\text{-PPh}_2)(CO)_{10}$, **5**, the orthometalated cluster complex $Os_3(\mu\text{-H})_2(\mu_3\text{-}\eta^3\text{-PPh}(C_6H_4))(CO)_9$, **6**, is formed (Scheme 2). **6** is known to add nucleophiles L to give $Os_3(\mu\text{-H})(\mu\text{-PPh}_2)(CO)_9L$ in high yield.[34] We heated **6** under ^{13}CO pressure. The resulting equilibrium between **5** and **6** gave after 5 h at 80 °C and subsequent chromatography ^{13}CO-enriched **5**. Comparison of the ^{13}C NMR spectra of the latter compound with a sample not enriched proves enrichment at all CO ligand positions. ^{13}CO-enriched **5** was subsequently deprotonated with DBU and converted to ^{13}CO-enriched **1a**, which was reacted with $HgCl_2$, giving a pure sample of ^{13}CO-enriched **2a**. A ^{13}C NMR spectrum of this cluster complex recorded in $CDCl_3$ at room temperature exhibited six resonances for the terminal CO ligands and one resonance for the bridging CO ligands. The observed number of resonances is most likely due to the above proposed intramolecular rotation of the Os_3 rings. For a rigid molecule **2a** nine resonances for the terminal CO ligands would have been expected. Obviously the rotation averages the chemical environment of the CO ligands perpendicular to the Os_3 planes, reducing the number of resonances to the observed value of six. Therefore we assume that the photocyclization process

Scheme 2

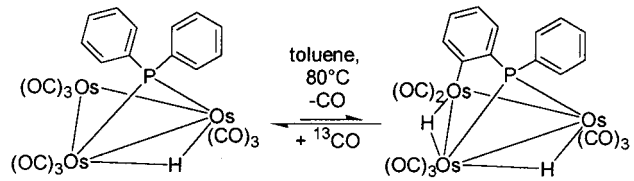

(33) Autorenkollektiv. *Photochemie*, VEB Deutscher Verlag der Wissenschaften: Berlin, 1975.

(34) Colbran, S. B.; Irele, P. T.; Johnson, B. F. G.; Lahoz, F. J.; Lewis, J.; Raithby, P. R. *J. Chem. Soc., Dalton Trans.* **1989**, 2023.

Scheme 3

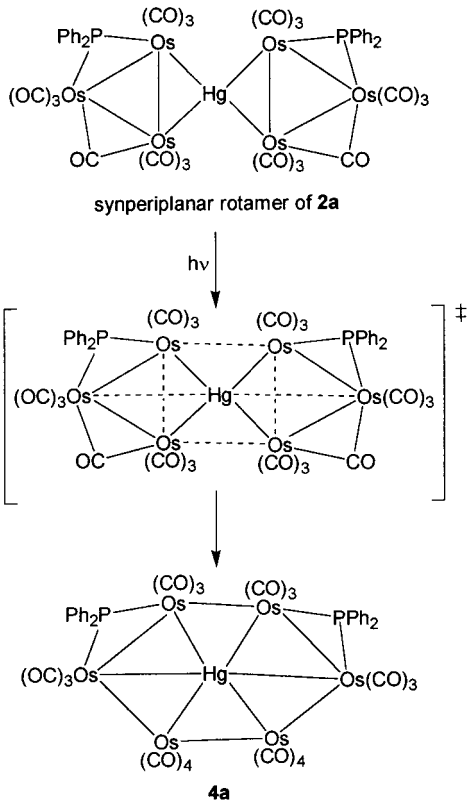

leading to **4a** and **4b**, respectively, is initiated when both Os_3 rings reach a synperiplanar orientation during the above-described rotational process since this orientation is preserved in **4a** and **4b** (Scheme 3). The photocyclization process is probably thermodynamically favored, as the number of metal−metal contacts increases from 10 in **2a** and **2b** to 12 in **4a** and **4b**.

Experimental Section

All reactions were performed in solvents free of oxygen that were dried according to literature methods, distilled, and stored under argon atmosphere. TLC was carried out on glass plates (20 × 20 cm^2) coated with a mixture of gypsum and silica gel (Merck 60 PF_{254}, 1 mm thick). The reaction products were characterized by ν(CO) FTIR spectroscopy (Nicolet P510, CaF_2 optics) and ^1H, ^{13}C, and ^{31}P NMR spectroscopy (Bruker AMX 300). UV/vis spectra were recorded with a Lambda 15 (Perkin-Elmer) spectrometer. The temperature of the cell was kept constant with a cryostat (MWG Lauda M3, accuracy ± 0.1 °C). Irradiation with polychromatic light was performed with a KL 1500 electronic (Schott) lamp. The intensity of the light was chosen to be 20% of the maximum intensity of the lamp for kinetic investigations and 40% of the maximum intensity for preparative reactions.

$HgCl_2$, [PPN]Cl (bis(triphenylphosphane)iminium chloride), and DBU (1,8-diazabicyclo[5.4.0]undec-7-ene) were purchased from Fluka and used as received. $Os_3(\mu\text{-H})_2(\mu_3\text{-}\eta^3\text{-PPh}(C_6H_4))(CO)_9$[34,35] and $Os_3(\mu\text{-H})(\mu\text{-PPh}_2)(CO)_{10}$ was prepared according to literature methods.[34] $Os_3(\mu\text{-H})(\mu\text{-P}(i\text{-Bu})_2)(CO)_{10}$ was prepared analogously to the latter compound from $Os_3(CO)_{11}(HP(i\text{-Bu})_2)$,[38,37] but this precursor was deprotonated with MeLi at −90 °C instead of DBU.

(35) Colbran, S. B.; Irele, P. T.; Johnson, B. F. G.; Lahoz, F. J.; Lewis, J.; Raithby, P. R. *J. Chem. Soc., Dalton Trans.* **1989**, 2033.
(36) Fajardo, M.; Holden, H. D.; Johnson, B. F. G.; Lewis, J.; Raithby, P. R. *J. Chem. Soc., Chem. Commun.* **1984**, 24.
(37) Johnson, B. F. G.; Lewis, J.; Pippard, D. A.. *J. Chem. Soc., Dalton Trans.* **1981**, 407.

Table 2. Selected Bond Lengths (Å) and Angles (deg)

		2a	
Hg1−Os1	2.8223(13)	Hg1−Os3	2.8542(15)
Hg1−Os4	2.8871(13)	Hg1−Os6	2.8109(15)
Os1−P1	2.318(6)	Os1−Os2	2.9483(15)
Os1−Os3	2.9738(13)	Os2−C7	2.30(2)
Os2−P1	2.331(6)	Os2−Os3	2.8937(14)
Os3−C7	2.07(2)	Os4−C14	1.99(2)
Os4−Os5	2.9252(16)	Os4−Os6	2.9510(13)
Os5−C14	2.28(2)	Os5−P2	2.325(5)
Os5−Os6	2.9623(12)	Os6−P2	2.311(6)
Os6−Hg1−Os1	126.17(4)	Os6−Hg1−Os3	156.69(5)
Os1−Hg1−Os3	63.18(3)	Os6−Hg1−Os4	62.37(3)
Os1−Hg1−Os4	155.53(5)	Os3−Hg1−Os4	119.37(4)
		3b	
Hg1−Os3	2.7971(9)	Hg1−Os4	2.8448(8)
Hg1−Os5	2.8518(10)	Hg1−Os1	2.8996(8)
Os1−C4	2.005(11)	Os1−Os2	2.8974(9)
Os1−Os3	2.9543(8)	Os2−C4	2.278(11)
Os2−P1	2.339(3)	Os2−Os3	2.9561(8)
Os3−P1	2.326(3)	Os4−P2	2.379(3)
Os4−Os6	2.8964(12)	Os4−Os5	2.9596(11)
Os5−P2	2.375(3)	Os5−Os6	2.8873(9)
Os5−Hg1−Os1	124.05(2)	Os5−Hg1−Os3	149.89(3)
Os1−Hg1−Os3	62.45(2)	Os5−Hg1−Os4	62.60(2)
Os1−Hg1−Os4	141.53(3)	Os3−Hg1−Os4	133.85(3)
		4a	
Hg1−Os1	2.8583(12)	Hg1−Os4	2.8598(13)
Hg1−Os2	2.8969(13)	Hg1−Os3	2.9097(13)
Hg1−Os6	3.0506(15)	Hg1−Os5	3.0683(13)
Os1−P1	2.332(5)	Os1−Os6	3.0874(13)
Os1−Os2	3.1023(15)	Os2−P1	2.313(5)
Os2−Os3	2.9656(12)	Os3−P2	2.294(5)
Os3−Os4	3.0865(13)	Os4−P2	2.320(6)
Os4−Os5	3.0767(14)	Os5−Os6	3.0576(14)
Os1−Hg1−Os4	172.80(4)	Os1−Hg1−Os2	65.23(3)
Os4−Hg1−Os2	121.90(4)	Os1−Hg1−Os3	122.24(4)
Os4−Hg1−Os3	64.68(3)	Os2−Hg1−Os3	61.42(3)
Os1−Hg1−Os6	62.90(3)	Os4−Hg1−Os6	110.11(4)
Os2−Hg1−Os6	127.69(4)	Os3−Hg1−Os6	152.68(4)
Os1−Hg1−Os5	110.98(4)	Os4−Hg1−Os5	62.41(3)
Os2−Hg1−Os5	152.16(4)	Os3−Hg1−Os5	126.47(4)
Os6−Hg1−Os5	59.96(3)		

Preparation of [PPN][$Os_3(\mu\text{-PR}_2)(CO)_{10}$] (R = Ph 1a, *i*-Bu 1b). In a Schlenk tube $Os_3(\mu\text{-H})(\mu\text{-PR}_2)(CO)_{10}$ (R = Ph, *i*-Bu) [100 mg; 0.964 mmol for R = Ph, 0.100 mmol for R = *i*-Bu] was dissolved in THF and treated with 1.1 equiv of DBU. The reaction mixture was stirred for 1 h, at which point 1 equiv of [PPN]Cl was added. Next the solvent was removed under reduced pressure and the orange residue taken up in 5 mL of methanol. On dropwise addition of water, a yellow precipitate formed, which was isolated by filtration and successively washed three times with water and hexane. The resulting orange solid was dried under reduced pressure, giving pure **1a** (133 mg, 87%) and **1b** (130 mg, 83%), respectively. Analytical and spectroscopic data: **1a** Anal. Calcd for $C_{58}H_{40}NO_{10}Os_3P_3$: C, 44.25; H, 2.56; N, 0.89. Found: C, 44.32; H, 2.43; N, 0.78. IR (CH_2Cl_2): $\nu_{C\equiv O}$ 2069 (sh), 2060 (w), 2004 (s), 1990 (vs), 1971 (m), 1942 (sh), 1928 (m). ^1H NMR ($CDCl_3$): 7.1−8.0 (m, Ph). ^{31}P NMR ($CDCl_3$): 21.7 (s, $[PPN]^+$); 76.2 (s, μ-PPh_2). **1b** Anal. Calcd for $C_{54}H_{48}NO_{10}Os_3P_3$: C, 42.27; H, 3.15; N, 0.91. Found: C, 42.15; H, 3.02; N, 0.85. IR (CH_2Cl_2): $\nu_{C\equiv O}$ 2052 (w), 2017 (sh), 1990 (vs), 1961 (m), 1936 (m), 1925 (m).

Reaction of [PPN][$Os_3(\mu\text{-PR}_2)(CO)_{10}$] (R = Ph 1a, *i*-Bu 1b) with $HgCl_2$. For this reaction daylight has to be entirely excluded. In a Schlenk tube 13.0 mg (0.048 mmol) of $HgCl_2$ was dissolved in 10 mL of THF and cooled to −90 °C. To the colorless solution was added an orange solution of **1a** (151 mg, 0.096 mmol) in 10 mL of THF. The resulting deep red solution was stirred for 10 min at −90 °C. Then the mixture was

Table 3. Crystallographic Data

	2a	2b	3b	4a
formula	$C_{44}H_{20}HgO_{20}Os_6P_2$	$C_{36}H_{36}HgO_{20}Os_6P_2$	$C_{36}H_{36}HgO_{20}Os_6P_2$·0.5pentane	$C_{44}H_{20}HgO_{20}Os_6P_2$·$CHCl_3$
fw	2272.3	2192.4	2228.4	2391.7
cryst syst	monoclinic	monoclinic	triclinic	triclinic
space group	$P2_1/c$	$P2_1/c$	$P\bar{1}$	$P\bar{1}$
temperature/K	293(2)	203(2)	203(2)	203(2)
a/Å	19.482(4)	22.005(4)	8.797(3)	10.459(4)
b/Å	15.934(3)	9.169(2)	11.403(2)	16.475(3)
c/Å	18.154(5)	25.072(3)	28.201(4)	16.676(4)
α/deg			84.76(2)	83.63(1)
β/deg	108.41(2)	91.45(1)	81.25(2)	87.55(1)
γ/deg			71.98(3)	82.58(1)
V/Å^3	5347.1(19)	5057.0(16)	2655.9(11)	2830.6(14)
Z	4	4	2	2
D_{calc}/g cm^{-3}	2.823	2.880	2.787	2.806
μ(Mo Kα)/mm^{-1}	17.19	18.17	17.30	16.38
F(000)	4040	3912	1998	2136
scan range *θ*/deg	2.0 to 27.5	2.7 to 27.5	2.7 to 27.5	2.5 to 27.0
no. of reflns	13 674/11 765	14 038/11 596	14 427/12 144	13 055/12 344
measd/unique R1[a]/wR2[b]	0.062/0.132	0.052/0.123	0.045/0.095	0.071/0.134
Goof	0.881	0.936	1.015	1.002
min./max. Δ*F*/e Å^{-3}	−0.84/0.96	−0.73/0.87	−1.21/1.38 near Os	−1.38/1.21 near Os

[a] $R1(F > 4\sigma(F)) = \sum||F_o| - |F_c||/\sum|F_o|$. [b] $wR2(F^2, \text{all data}) = [\sum w(F_o^2 - F_c^2)^2/\sum w(F_o^2)^2]^{1/2}$.

warmed to 0 °C and the solvent removed at reduced pressure. The red residue was subjected to TLC separation using CH_2Cl_2/hexane (2:1) as eluent. Two main bands (violet, higher R_f value, and red, lower R_f value) were developed, but did not completely separate. The head of the violet band and the tail of the red band were worked up. According to ^{31}P NMR spectra the violet fraction mainly consists of **3a** and small amounts of **4a**, whereas the red fraction mainly consists of **2a** and smaller amounts of **3a** and **4a**. From the violet fraction pure **3a** in a yield of about 15 mg (13%) was isolated by fractional crystallization from 1,4-dioxane. From the red fraction pure **2a** in a yield of about 40 mg (37%) and **4a** in a yield of about 7 mg (6%) were isolated by fractional crystallization from *n*-hexane/$CHCl_3$. The fraction between head and tail was isolated as well and consists of a mixture of **2a**, **3a**, and **4a**. Since all of the isolated cluster complexes have the same molecular mass their overall yield was easily determined to be 78 mg (71%).

The reaction of **1b** (148 mg, 0.096 mmol) with $HgCl_2$ was performed analogously to the above-described reaction except pure **3b** was obtained by crystallization of the violet fraction from *n*-hexane/$CHCl_3$. The overall yield in this case was 80 mg (76%).

Analytical and Spectroscopic Data. 2a Anal. Calcd for $C_{44}H_{20}HgO_{20}Os_6P_2$: C, 23.26; H, 0.89. Found: C, 22.99; H, 0.83. IR (CH_2Cl_2): $\nu_{C\equiv O}$ 2108 (vw), 2091(m), 2067 (vw), 2056 (m), 2031 (vs), 2009 (m), 1999 (w), 1981 (w), 1973 (m), 1803 (vw). ^{1}H NMR ($CDCl_3$): 7.0−8.0 (m, Ph). ^{13}C NMR ($CDCl_3$) (^{13}CO-enriched sample, CO region): 177.9 (d, $J_{PC} = 6$ Hz), 178.3 (d, $J_{PC} = 5$ Hz), 180.9 (s), 182.7 (s), 184.0 (s), 186.4 (s), 205.7(d, $^2J_{PC} = 15$ Hz, *μ*-CO). ^{31}P NMR ($CDCl_3$): 216.6 (s, *μ*-P). **2b** Anal. Calcd for $C_{36}H_{36}HgO_{20}Os_6P_2$: C, 19.72; H, 1.66. Found: C, 19.83; H, 1.45. IR (CH_2Cl_2): $\nu_{C\equiv O}$ 2108 (vw), 2092 (w), 2058 (m), 2046 (m), 2025 (vs), 1981 (m), 1967(sh), 1813 (w). ^{1}H NMR ($CDCl_3$): 1.2−2.5 (m, *i*-Bu). ^{31}P NMR ($CDCl_3$): 189.1 (s, *μ*-P). **3a** Anal. Calcd for $C_{44}H_{20}HgO_{20}Os_6P_2$: C, 23.26; H, 0.89. Found: C, 23.41; H, 0.95. IR (CH_2Cl_2): $\nu_{C\equiv O}$ 2112 (w), 2096 (vw), 2075 (sh), 2069 (m), 2054 (m), 2027 (vs), 1998 (m), 1975-(m), 1963 (sh), 1813 (vw). ^{1}H NMR ($CDCl_3$): 6.7−8.0 (m, Ph). ^{31}P NMR ($CDCl_3$): 43.9 (s, *μ*-P), 209.7 (s, *μ*-P). **3b** Anal. Calcd for $C_{36}H_{36}HgO_{20}Os_6P_2$: C, 19.72; H, 1.66. Found: C, 19.92; H, 1.33. IR (CH_2Cl_2): $\nu_{C\equiv O}$ 2112 (w), 2094 (vw), 2070 (m), 2054 (m), 2030 (vs), 1998 (m), 1968(m), 1963 (sh), 1815 (vw). ^{1}H NMR ($CDCl_3$): 1.2−2.6 (m, *i*-Bu). ^{31}P NMR ($CDCl_3$): 23.9 (s, *μ*-P), 195.7 (s, *μ*-P). **4a** Anal. Calcd for $C_{44}H_{20}HgO_{20}Os_6P_2$: C, 23.26; H, 0.89. Found: C, 23.13; H, 0.88. IR (CH_2Cl_2): $\nu_{C\equiv O}$ 2114 (w), 2071 (vs), 2054 (m), 2025 (vs), 2011 (m), 1998 (m), 1973 (sh), 1967 (m). ^{1}H NMR ($CDCl_3$): 7.1−8.1 (m, Ph). ^{31}P NMR ($CDCl_3$): 85.4 (s, *μ*-P). **4b** Anal. Calcd for $C_{36}H_{36}HgO_{20}Os_6P_2$: C, 19.72; H, 1.66. Found: C, 19.95; H, 1.56. IR (CH_2Cl_2): $\nu_{C\equiv O}$ 2110 (w), 2069 (s), 2063 (vs), 2019 (s), 2005 (w), 2046 (s), 1990 (m), 1973 (w), 1967 (w). ^{1}H NMR ($CDCl_3$): 1.2−2.8 (m, *i*-Bu). ^{31}P NMR ($CDCl_3$): 54.5 (s, *μ*-P).

Preparative Photochemical Conversion of μ_4-Hg[Os_3-(μ-PPh_2)(μ-CO)$(CO)_9$]$_2$ (2a) to Os_6(μ-Hg)(μ-PPh_2)$_2(CO)_{20}$ (4a). In a 150 mL Schlenk tube 92 mg (0.04 mmol) **2a** was dissolved in 40 mL of THF. The solution was stirred and simultaneously irradiated by polychromatic light at room temperature. The course of the reaction was followed by analytical TLC. When almost all of **2a** had reacted, the solvent was removed under reduced pressure and the red residue subjected to TLC with CH_2Cl_2/hexane (2:1) as eluent. A tiny red band of educt **2a** (higher R_f value) and a large red band containing **4a** developed. In addition a large gray band of decomposition products was observed on the starting spot. From the first band 7 mg (8%) of **2a** was isolated. **4a** was isolated from the main band in a yield of 48 mg (53%).

Preparation of ^{13}CO-Enriched Os_3(μ-H)(μ-PPh_2)$(CO)_{10}$ (5). In a glass autoclave 190 mg (0.188 mmol) of $Os_3(\mu\text{-H})_2(\mu_3\text{-}\eta^3\text{-PPh}(C_6H_4))(CO)_9$, **6**, was dissolved in 25 mL of toluene under an argon atmosphere. Subsequently the vessel was closed, and 0.5 bar ^{13}CO was added. Now the solution was heated to 80 °C and stirred at this temperature for 5 h. After cooling to room temperature the overpressure was let off and the orange solution was transferred into a flask. Reduced pressure was then applied to remove the solvent. The orange residue obtained was 182 mg (96% yield) of ^{13}CO-enriched Os_3(μ-H)-(μ-PPh_2)$(CO)_{10}$ (**5**). The exact degree of enrichment was not determined, but comparison with ^{13}C NMR spectra of not enriched **5** exhibited that enrichment with approximately the same degree had taken place at all CO ligand positions. Anal. Calcd for $C_{12}(^{13}C)_{10}H_{11}O_{10}Os_3P$: C, 26.17; H, 1.05. Found: C, 25.98; H, 1.22. IR (CH_2Cl_2): $\nu_{C\equiv O}$ 2100 (m), 2054 (vs), 2047 (sh), 2017 (s), 1986 (m), 1976 (sh), 1950 (vw). ^{1}H NMR ($CDCl_3$): −18.07 (d, $^2J_{PH} = 19.7$ Hz, 1H, *μ*-H), 6.72−7.91 (m, 10H, Ph) ppm. ^{13}C NMR ($CDCl_3$): C(Ph): 127.5 (d, $J_{CP} = 11$ Hz), 128.8 (s), 129.0 (d, $J_{CP} = 12$ Hz), 131.3 (d, $^1J_{CP} = 53$ Hz, C^1), 131.4 (d, $J_{CP} = 3$ Hz), 132.4 (d, $J_{CP} = 11$ Hz), 136.1 (d, $J_{CP} = 10$ Hz), 145.9 (d, $^1J_{CP} = 43$ Hz), C (CO): 172.2 (d, $^2J_{CP} = 7$ Hz), 173.0 (d, $^2J_{CP} = 8$ Hz), 173.6 (s (broad)), 177.6 (s), 178.4 (s), 180.2 (d, $^2J_{CP} = 8$ Hz). ^{31}P NMR ($CDCl_3$): 16.1 (s, *μ*-P).

Crystal Structure Determinations. Crystals suitable for X-ray analysis for compounds **2a**, **2b**, **3b**, and **4a** were obtained from chloroform/pentane solutions. Despite various attempts

for **4a** only crystals of minor quality and scattering power could be gained.

Pertinent crystallographic data are summarized in Table 3. All data sets were collected on a Bruker AXS P4 diffractometer with graphite-monochromated Mo Kα radiation. Standard reflections monitored after every 400 reflections showed a decrease of 1−2% for **2a**, **2b**, and **4a** and of 9% for **3b**, respectively. The intensities of the data sets were corrected accordingly. Intensities of all data sets were corrected for Lorentz−polarization effects, and absorption corrections via ψ-scans were applied. The structures were solved by direct and conventional Fourier methods. Full-matrix least-squares refinement was based on F^2. All but hydrogen atoms were refined anisotropically; geometrically placed hydrogen atoms were refined with a riding model and $U(H) = 1.2\ U(C_{iso})$ and $1.5U(C_{iso})$ for methyl-C. Programs used for calculations: SHELX-97.[39]

UV/Vis Kinetics of the Rearrangement 2a → 3a. All important data are summarized in Table 1. The scan rate of all spectra recorded was 240 nm min^{-1}. At higher temperatures the measuring range was reduced in order to get a sufficient number of spectra. The measurements were performed under complete exclusion of daylight and were ended long before conversion of **2a** to **3a** was complete, as at longer periods of time secondary reactions occurred, making the evaluation of the obtained data impossible. Subsequently periodically occurring errors in measurement were eliminated according to literature methods.[40] The resulting reduced sets of data were analyzed by formal integration,[32] giving the rate constants at each temperature. The temperature dependence of the rate constants was evaluated by an Eyring plot,[41] leading to the thermodynamic parameters of activation at $T = 298.2$ K (Table 1). The mean deviation of these parameters was determined according to Gauss's law of propagation of error.

Photochemical Rearrangement 2a → 4a. The reaction was monitored by UV/vis spectroscopy at 5 °C in THF from 190 to 700 nm with a scan rate for each spectrum of 60 nm min^{-1}. The concentration of **2a** amounted to 0.0426 mmol L^{-1}. After the recording of each spectrum the cuvette was irradiated with polychromatic light for 60 s. Then the next spectrum was recorded. This procedure was repeated six times. Eventually in order to complete conversion, the curette was irradiated with more intense polychromatic light for 10 min. The final spectrum recorded is identical with a spectrum of a solution of pure **4a**.

Supporting Information Available: Refined atomic coordinates, bond lengths and angles, anisotropic thermal parameters, and calculated hydrogen atomic coordinates for **2a**, **2b**, **3b**, and **4a**. This material is available free of charge via the Internet at http://pubs.acs.org.

OM0110585

(38) Drake, S. R.; Khattar, R. *Organomet. Synth.* **1988**, *4*, 234.

(39) Sheldrick, G. M. *SHELX-97*, A Program for Crystal Structure Solution and Refinement; University of Göttingen, 1998.

(40) Swinbourne, E. S. *Auswertung und Analyse kinetische Messungen*; Verlag Chemie: Weinheim, 1975.

(41) Wedler, G. *Lehrbuch der physikalischen Chemie*, 4.Auflage; VCH-Wiley: Weinheim, 1997.

(42) Egold, H.; Schraa, M.; Flörke, U., unpublished results.